9th 2023

ICNTC CONFERENCE

INTERNATIONAL CONFERENCE ON NEW TRENDS IN CHEMISTRY

9th INTERNATIONAL CONFERENCE ON
NEW TRENDS IN CHEMISTRY
19 – 21 MAY 2023

9th ICNTC PROCEEDINGS BOOK

9th INTERNATIONAL CONFERENCE ON NEW TRENDS IN CHEMISTRY

19-21 MAY 2023 | Skopje, North Macedonia

ICNTC CONFERENCE
INTERNATIONAL CONFERENCE ON NEW TRENDS IN CHEMISTRY

9th INTERNATIONAL CONFERENCE ON NEW TRENDS IN CHEMISTRY
16 – 18 MAY 2022

19 – 21 MAY 2023

http://www.icntcconference.com/

ICNTC Conference 2023

9th International Conference on New Trends in Chemistry

Published by the ICNTC Secretariat
Editor:
Prof. Dr. Dolunay ŞAKAR DAŞDAN

ICNTC Secretariat
Büyükdere Cad. Ecza sok. Pol Center 4/1 Levent-İstanbul
E-mail: icntcconference@gmail.com
http://www.icntcconference.com

Conference organised in collaboration with Monre Academy

ISBN: 978-605-73406-2 -7

SCINTIFIC COMMITTEE

Prof. Dr. Janusz Stafiej,
Cardinal Stefan Wyszynski University, Warsaw, Poland

Prof. Dr. Dolunay Sakar Dasdan,
Yıldız Technical University, Turkey
Conference Chair

PhD Dr. Habil. Agnieszka Kaczor,
Medical University of Lublin, Poland

PhD Dr. Habil. Agata Bartyzel,
University of Maria Curie-Sklodowska, Poland

PhD Dr. Habil. Daniel Ayuk Mbi Egbe,
Linz Institute for Organic Solar Cells, Austria

Dr. Eduardo V. Ludeña,
Escuela Superior Politecnica del Litoral Ecuador

Dr. Hatem M.A. Amin
Faculty of Chemistry and Biochemistry, Ruhr-University Bochum, Germany

Dr. Mauricio Heriberto Cornejo Martinez,
Escuela Superior Politecnica del Litoral Ecuador

PhD Pabitra Saha
RWTH Aachen University, Aachen, Germany

PhD Flavio Massignan
Eötvös Lorand University, Budapest,Hungary

ORGANIZATION COMMITTEE

Prof. Dr. Dolunay Sakar Dasdan
Yıldız Technical University – Turkey
Conference Chair

Prof. Dr. Yelda Yalcin Gurkan
Namik Kemal University – Turkey
Chemistry Department

Dear Colleagues,

I am honoured to invite and send you this call for papers on behalf of Conference Organisation Board of "9**th International Conference on New Trends in Chemistry**", to be held in Skopje, North Macedonia on the dates between May 19 – 21 , 2023

Limited number of Papers and Posters with the below mentioned topics will be accepted for our conference:

- Polymer Chemistry and Applications
- Pharmaceutical Chemsitry
- Computational Chemistry
- Bio Chemistry
- Physical Chemistry
- Analytical Chemistry
- Inorganic Chemistry
- Organic Chemistry
- Material Chemistry
- Environmental Chemistry
- Food Chemistry

The selected papers which are presented as oral in the conference will be published in an international peer-reviewed journal which is indexed by SCOPUS as Q4. Each manuscript will have doi Numbers.

We kindly wait for your attendance to our conference to be held on 19 – 21 May 2023,

All informations are available in conference web site. For more information please do not hesitate to contact us. info@icntcconference.com

Respectfully Yours,

On Behalf of the Organization Committee of ICNTC Conference

Prof. Dr. Dolunay SAKAR DASDAN
9th ICNTC 2023 | Conference Chair
Yıldız Technical University – Istanbul / Turkey
Chemistry Department

19 MAY 2023 FRIDAY

10:00 – 10:10
Welcome Speech : **Prof. Dr. Dolunay SAKAR/** Conference Chair
Yıldız Technical University, Turkey

10:10 – 11:00
Keynote Speech : **Prof. Dr. Heikki TENHU**
Speech Title : Polyelectrolytes – water soluble or not

SESSION A

SESSION CHAIR	**Prof. Dr. Sevil YUCEL**	
TIME	**PAPER TITLE**	**PRESENTER** / CO AUTHOR
11:00 – 11:20	HIGH RATE PROTOLYSIS ATTRACTORS ACTIVATE energy over zero $G_{(Pt)=GH2O}$=G_{CO2gas}=0 kJ/mol of indifferent (Pt), water and carbon dioxide FREE ENERGY CONTENT as BIOSPHERE Self-ORGANIZATION for PERFECT ORDER IRREVERSIBLE HOMEOSTASIS SUSTAINING the PROGRESS of BIOENERGETIC, EVOLUTION and SURVIVAL	**Aris KAKSIS**
11:20 – 11:40	VISIBLE LIGHT-DRIVEN PHOTOCATALYTIC HYDROGEN EVOLUTION ON DYE-SENSITIZED BISMUTH PHOSPHATE	**Gizem YANALAK**, Kübra Turgut, Adem Sarılmaz, Faruk Ozel, İmren Hatay Patır, Mustafa Ersöz
11:40 – 12:00	EFFECT OF NITROGEN FERTILIZER APPLICATION ON PLANT USABLE NITROGEN SPECIES IN SOIL DURING SORGHUM GROWING SEASON ON MARGINAL LANDS IN ONTARIO, CANADA	**Julia LU**
12:00 – 12:20	EXAMINATION OF THE CATALYTIC EFFECT OF CARBON DERIVATIVE METALLIC NANOMATERIALS ON POLLUTANTS IN WATER	**Didem AYDIN**, Ilkay Hilal GUBBUK, Mustafa ERSOZ
12:20 – 12:40	A SURFACE NETWORK BASED ON OXIDATIVE GRAPHENE OXIDE FOR THE DETERMINATION OF HYDROQUINONE AND CATECHOL IN GROUND AND WASTEWATER SAMPLES	**Emad A. Khudaish**
12:40 – 13:00	PREPARATION AND CHARACTERIZATION OF POLYSACCHARIDE BASED ORAL FILMS FOR QUETIAPINE FUMARATE RELEASE	**Merve YAMAN AGIRMAN**, Ilknur KUCUK

13:00 – 14:00	**LUNCH B R E AK** **LUNCH IS NOT INCLUDED INTO REGISTRATION FEE**

SESSION B

SESSION CHAIR	**Prof. Dr. Nuriye AKBAY**	
TIME	**PAPER TITLE**	**PRESENTER** / CO AUTHOR
14:00 – 14:20	DEGREDATION REACTION KINETIC OF 6-APA	**Seyda AYDOGDU**, Arzu Hatipoglu
14:20 – 14:40	DETERMINATION OF PHYSIOCHEMICAL PROPERTIES OF PRIMARY METABOLITES OF AN ANTIDEPRESSANT DRUG BY MOLECULAR MODELING	**Simal KURUMOGLU**, Yelda YALÇIN GÜRKAN
14:40 – 15:00	CALCULATING ANALYSIS OF SEASONAL CHANGES AND DEGRADATION REACTIONS OF PESTICIDES IN SURFACE WATERS FEEDING SÜLEYMANPAŞA DISTRICT, TEKİRDAĞ	**Cigdem SAYIKLI SIMSEK**, Yelda YALCIN GURKAN
15:00 – 15:20	SCREENING OF SUPPORTED BIMETALLIC Fe CATALYSTS FOR LIGHT OLEFIN PRODUCTION in FTS: EFFECT OF SUPPORT MATERIALS	**Deniz UYKUN MANGALOGLU**, Hüsnü ATAKÜL
15:20 – 15:40	A STUDY TO UNDERSTAND THIOFLAVIN-T INTERACTION WITH AB PEPTIDES AND FIBRILS	**Pelin GUZEL, Dila KAYA, Nuriye AKBAY**

15:40 – 16:00	**B R E AK**

SESSION C – POSTER SESSION

SESSION CHAIR	**Prof. Dr. Julia LU, Prof. Dr. Sevil YUCEL**	
TIME	**PAPER TITLE**	**PRESENTER** / CO AUTHOR
16:00-17:00	SYNTHESIS OF CNT BASED METALLIC NANOPARTICLES AS EFFECTIVE CATALYSTS FOR THE DEGRADATION OF ORGANIC POLLUTANTS WITH $NABH_4$ IN WATER	**Ilkay Hilal GUBBUK**, Didem AYDIN, Mustafa ERSOZ
	DEVELOPMENT OF METAL ORGANIC FRAMEWORK BASED MEMBRANES AND THEIR APPLICATION	Gülcihan ÖZDEM, Mustafa ERSÖZ**, İlkay Hilal GUBBUK,** Özlem ALTINTAŞ YILDIRIM, Hakan ERER
	DYE-SENSITIZED CALCIUM TUNGSTATE ($CaWO_4$) STRUCTURE FOR	**Imren Hatay PATIR**, Kübra Turgut, Gizem Yanalak, Adem Sarılmaz, Faruk Ozel, Mustafa

	PHOTOCATALYTIC HYDROGEN GENERATION WITH VISIBLE LIGHT	Ersöz
	REMOVAL of PYRACLOSTROBIN, PINOXADEN, GAMMA-CYHALOTHRIN PESTICIDES FROM GROUNDWATER BY DFT METHOD	Hidayet GUREL YORULMAZ, Burak GURKAN, **Yelda YALCIN GURKAN**
	ELECTRONIC PROPERTIES OF PLATIN-BASED ANTICANCER DRUGS	Mert Evirgen, Seyda Aydogdu, **Arzu HATIPOGLU**
	$LaNiO_3$ CATALYSED AMINATION OF PHENOLS	**Anna Adel ADAM**, Sándor Balázs NAGY, Szilveszter ZIEGENHEIM, Pál SIPOS, Gábor VARGA
	SYNTHESIS AND CHARACTERIZATION OF POLY(ETHYLENE-ALT-MALEIC-ANHYDRIDE)-PREGABALIN (1:1) RATIO CONTROLLED DRUG DELIVERY SYSTEM WITH CATALYST FREE MEDIA	**Ozge ESLEK,** Dolunay ŞAKAR
	CHOOSING A SECOND ADSORBENT TO SAMPLE VOLATILE ORGANIC COMPOUNDS IN BIOMASS GASIFICATION TAR	**Aleksandrs I. PUCKINS**, Sergejs D. OSIPOVS
	EFFECT OF ANIONIC/NONIONIC EMULGATOR SYSTEMS ON THE PROPERTIES OF WATER BASED STYRENE/ACRYLIC COPOLYMER PAINT BINDERS	Berfin Ceyda AYHAN, **Dolunay SAKAR**, Emine Cansu TARAKÇI
	CHEMICAL PVA HYDROGELS AS CLEANING DEVICE OF ANCIENT SURFACES	**Martina REDI,** Ozge ESLEK, Ester CHIESSI, Fabio DOMENICI, Gaio PARADOSSI
	COMPARATIVE TECHNO-ECONOMIC ANALYSIS OF INDUSTRIAL-SCALE BIOBUTANOL PRODUCTION PROCESSES FOR AN EFFICIENT WASTE MANAGEMENT	**Abdullah Bilal OZTURK** , Tulin OZBEK ,

SESSION D – POSTER SESSION

SESSION CHAIR	**Assoc. Prof. Dr. Emel AKYOL, Assoc. Prof. Dr. Azmi Seyhun KIPCAK**	
TIME	**PAPER TITLE**	**PRESENTER** / CO AUTHOR
17:00-18:00	STUDY OF THE TOXICITY OF BENZANTHRONE LUMINESCENT DYES	**Jelena KIRILOVA**, Marina SAVICKA, Alise KIRILOVA, Armands MALECKIS, Tatjana GRIGORJEVA
	ANALYTICAL METHOD FOR THE DETERMINATION OF TAR PRODUCED	**Sergejs D. OSIPOVS**, Aleksandrs I. PUČKIN

	FROM THE PYROLYSIS OF WASTE TYRES	
	EVALUATION OF NOVEL DESIGNED DELICIOUS PEPTIDES FOR IMPROVING TASTE SENSATION	Ahmet Cenk ANDAÇ, **Sevil YUCEL**, Cem ÖZEL, Ceren KEÇECİLER , Kevser KÖKLÜ
	SYNTHESIS AND CHARACTERIZATION OF COBALT SULFIDE LAYERS	**Asta BRONUSIENE**, Skirma ZALENKIENE, Ingrida ANCUTIENE, Remigijus IVANAUSKAS
	SYNTHESIS AND CHARACTERIZATION OF TIN SULFIDE NANOPARTICLES	**Asta BRONUSIENE**
	ASSESSMENT OF OXIDATIVE STRESS BY DETECTION OF H_2O_2 IN RYE SAMPLES USING A MULTIELECTRODE ELECTROCHEMICAL SENSOR	**Irena MIHAILOVA**, Vjaceslavs GERBREDERS, Marina KRASOVSKA, Valdis MIZERS, Eriks SLEDEVSKIS
	CONVOLUTIONAL NEURAL NETWORK-BASED EVALUATION OF CHEMICAL MAPS OBTAINED BY FAST RAMAN IMAGING FOR PREDICTION OF TABLET DISSOLUTION PROFILES	**Boldizsár ZSIROS**, Dorián László GALATA, Gábor KNYIHÁR, Orsolya PÉTERFI, Lilla Alexandra MÉSZÁROS, Ferenc RONKAY, Brigitta NAGY, Edina SZABÓ, Zsombor Kristóf NAGY, Attila FARKAS
	THE IMPACT OF STRUCTURE OF SELECTED CATIONIC LIPIDS ON PHYSICOCHEMICAL PROPERTIES OF MODEL MAMMALIAN MEMBRANES	**Marzena MACH**, Paweł WYDRO
	EFFECT OF ALKALINE EARTH IONS ON THE BEHAVIOUR OF ALKYLBENZENE SULFONATES	**Szilveszter ZIEGENHEIM**, Anna Adél ÁDÁM, Csaba BÚS, Bence KUTUS, Pál Sipos, László JANOVÁK, Imre DÉKÁNY

18:45 – 22:00	**GALA DINNER** **Participants who registered as FULL PACKAGE has free Access to Dinner**

20 MAY 2023 SATURDAY

10:20 – 11:00
Keynote Speech **: Prof. Dr. Sefik SUZER**
Speech Title **:** XPS, A Chemical Analysis Tool for Exploring Electrical Properties of Liquid/Solid Interfaces

SESSION E

SESSION CHAIR	**Assoc. Prof. Dr. Emel AKYOL**	
TIME	**PAPER TITLE**	**PRESENTER** / CO AUTHOR
11:00 – 11:20	EFFECTS OF ALCOHOLS ON SODIUM DODECYLSULPHATE'S SOLUTION CHEMISTRY PROPERTIES AND DISSOLUTION OF $CASDS_2$ PRECIPITATES	**Csaba BUS,** Pál Sipos, Bence Kutus
11:20 – 11:40	DNA BINDING STUDIES FOR SOME SMALL MOLECULES	**Ayşegül GOLCU**
11:40 – 12:00	EFFECTS OF DRYING METHODS ON THE DRYING KINETICS OF BLANCHED BROWN CRAB MEAT	Zehra Ozden OZYALCIN**, Azmi Seyhun KIPCAK**
12:00 – 12:20	PHOTOCATALYTIC ACTIVITY of TiO_2-Cu-METAL-ORGANIC FRAMEWORK (MOF)	Ayşenur KATIRCI, M. Efgan KİBAR, **Filiz UGUR NIGIZ**
12:20 – 12:40	PERVAPORATIVE DESALINATION BY PHOSPHOMOLYBDIC ACID/PVA HYBRID MEMBRANE	**Derya UNLU**
12:40 – 13:00	THE EFFECT OF ULTRASOUND PRETREATMENT ON THE OVEN AND VACUUM OVEN DRYING KINETICS OF BLUEBERRIES	Zeyd Emin TAŞÇI, **Ekin KIPCAK**

13:00 – 14:00	**LUNCH B R E AK** **LUNCH IS NOT INCLUDED INTO REGISTRATION FEE**

SESSION F

SESSION CHAIR	**Prof. Dr. Aysegul GOLCU**	
TIME	**PAPER TITLE**	**PRESENTER** / CO AUTHOR
14:00 – 14:20	POLYSACCAHARIDE BASED FILMS FOR A TRANSDERMAL DRUG DELIVERY SYSTEMS	**Deniz EKSI**, İlknur KÜÇÜK

14:20 – 14:40	ZR-BASED METAL ORGANIC FRAMEWORK FILLED MEMBRANE SYNTHESES AND APPLICATION FOR CO_2/N_2 SEPARATION	**Filiz UGUR NIGIZ**
14:40 – 15:00	2-(((3-CHLOROPHENYL)IMINO)METHYL)-4-NITROPHENOL: SYNTHESIS, MOLECULAR AND MEDICINAL STUDIES	**Songul SAHIN**, Necmi Dege
15:00 – 15:20	POLYACRYLIC ACID AND POLYACRYLIC ACİD SODIUM SALT AS INHIBITORS OF CALCIUM OXALATE CRYSTAL FORMATION	Ahmed sadeq Abdo Esmail AL-DUBAI, **Emel AKYOL**

15:20 – 16:00	**COFFEE B R E AK**

16:00 – 16:30	**CLOSING CEREMONY**

21 MAY 2023 SUNDAY

	FREE DAY

Contents

HIGH RATE PROTOLYSIS ATTRACTORSACTIVATE ENERGY OVER ZERO $G_{H2O}=G_{CO2GAS}=0$ $^{KJ}/_{MOL}$ OF WATER AND CARBON DIOXIDE. FREE ENERGY CONTENT AS BIOSPHERE SELF-ORGANIZATION CREATES PERFECT ORDER IRREVERSIBLE HOMEOSTASIS PROGRESS OF BIOENERGETIC, EVOLUTION AND SURVIVAL.

Aris Kaksis,

Riga Stradin's University, dep. Human Physiology and Biochemistry aris.kaksis@rsu.lv,

Abstract. The quantitative studies for oxygen, carbon dioxide and water protolysis functional activity reveal multiply generated Self-Organization Attractors: water [H_2O]=55.3 $^{mol}/_{Liter}$ concentration, pH=7.36, enzyme Carbonic Anhydrase reactivity, air oxygen level 20.95 %, osmolar concentration 0.305 M, ionic strength 0.25 M, temperature 310.15 K degree etc.[1] High rate protolysis in water make oxygen fire safe , functionally activate $\mathbf{CO_{2aqua}}$ for Life Homeostasis. In 2023rd have to note hundred years since Brønsted - Lowry protolysis, which high rate protonation stay at equilibria while other reactions continues as much more slower. Arterial dissolute oxygen concentration [$\mathbf{O_{2aqua}}$]=6*10^{-5} Makes safe Bioenergetic sustaining isooxia with air oxygen level 20.95 % is the Attractor 500 MYears. [6,14]

The perfect order irreversible non-equilibrium reactions of Homeostasis are created by activation with high rate protolysis Attractors, which stay at equilibrium and activate molecules for progress of Homeostasis. Those indispensably are for irreversible continuing Homeostasis. Homeostasis generates bioenergetic concentration gradients for transport down and for osmosis against the gradients, which as Brownian molecular engines drive the organism Homeostasis for evolution and for survival. [2,3,4] Deviation from high rate protolysis Attractors values disorder the Self-Organization perfect reaction order of Homeostasis. The nascent Chaos disorders and stops the Homeostasis which disappears as extinct from Biosphere. Zero energy $G_{e^-}=G_{H2O}=G_{CO2gas}=0$ $^{kJ}/_{mol}$ to free electrons e^-, for water $\mathbf{H_2O}$ and $\mathbf{CO_{2gas}}$ bases on Hydrogen $G_{H2gas}=\mathbf{85.6}$ $^{kJ}/_{mol}$ in water $G_{H2aqua}=\mathbf{103}$ $^{kJ}/_{mol}$ and metal $\mathbf{G_{H(Pt)}}=51$ $^{kJ}/_{mol}$. [8]

Key Words: *Biochemistry; Physical Chemistry; Thermodynamics; Protolysis; Attractors.*

1. Introduction.

In 1977th[4] declares: equilibrium state is Attractor for non-equilibrium states in plural reactions and mixtures of compounds. Scientist [3,4] explains perfect order of reactions formation in Universe and Sciences as Self-Organization Attractors.

About Universe creation in perfect order Maria Kuman: „The nonlinear no equilibrium theory of Scientist [4] is also called The Chaos Theory because it claims that our Universe was created in perfect order out of the chaos.". [5] Chaos is just apparent disorder. The Biosphere Homeostasis belongs to our human civilization and is best studied perfect part of Universe.

2. High rate protolysis Attractors create irreversible perfect order progress of Homeostasis.

Homeostasis products $G_{H2O}=G_{CO2gas}=0$ level zero free energy compounds water and carbon dioxide gas in Hess law free energy of formation are negative $G°_{H2O}$=-237.19 $^{kJ}/_{mol}$, $G°_{CO2gas}$=-394.36 $^{kJ}/_{mol}$. [1]

Alberty [8] free energy for Hydrogen gas G_{H2gas}=85.64 $^{kJ}/_{mol}$ lets determinate oxygen G_{O2aqua}=330 $^{kJ}/_{mol}$, carbon G_{gr}=91.26 $^{kJ}/_{mol}$, peroxide G_{H2O2}=364.8 $^{kJ}/_{mol}$ and glucose $\mathbf{G_{C6H12O6}}$=2268.8 $^{kJ}/_{mol}$ in Biochemical potential scale relative to zero background values of water and carbon dioxide gas $G_{H2O}=G_{CO2gas}=0$ $^{kJ}/_{mol}$.

1)Free energy from gas to solubility in water increases $G_{O2aqua}=G_{O2gas}+G_{O2sp}$=303.1+26.58=330 $^{kJ}/_{mol}$ as low solubility constant $\mathbf{O_{2gas\ AIR}}+\mathbf{H_2O}\xrightarrow{Aquaporins}\mathbf{O_{2aqua}}$ value $\mathbf{K_{sp}}=\frac{[O_{2\ aqua}]}{[O_{2\ gas}]\cdot[H_2O]}$=2.205*10^{-5} the free energy increases about $G_{O2sp}=\mathbf{-R•T•ln(K_{sp})}$=-8.3144*298.15*ln(2.205*10^{-5})=26.58 $^{kJ}/_{mol}$. [14]

$O_{2aqua}+4H_3O^+ +4e^- <=> 6H_2O$ thermodynamic standard potential $E°_{O2}$=1.485 V create arterial potential $E_{O2}=E°_{O2}+{}^{0.0591}/_{4}\bullet\log([O_{2aqua}]\bullet[H_3O^+]^4/_{[H2O]^6})=1.485+{}^{0.0591}/_{4}*\log(6*10^{-5}*10^{-7.36*4}/_{55.346\wedge 6})$=0.833 Volts .

$\Delta E_{arterial}=E°_{O2}-E_{O2}$=-1.485+0.833=-0.652 V change $\Delta G_{arterial}=\Delta E_{arterial}*F*n$=-0.652*96485*4/1000=-251.6 $^{kJ}/_{mol}$.

Protolysis free energy $G_{O2Biochem\_arterial}=G_{O2gas}+G_{O2sp}+\Delta G_{arterial}$=303.1+26.58-251.6=78.08 $^{kJ}/_{mol}$ decreases and oxygen becomes fire safe biochemical oxidant, forming arterial concentration [$\mathbf{O_{2aqua}}$]=6*10^{-5} M isooxia as normal safe progress of Bioenergetic.

2) CA generates free energy content from zero $G_{CO2+2H2O}=0$ $^{kJ}/_{mol}$ to $G_{H3O+HCO3-}$=68.4 $^{kJ}/_{mol}$.

Zero level $\mathbf{CO_{2gas}}+\mathbf{H_2O}<=>\mathbf{CO_{2aqua}}$ to aqua $G_{spCO2aqua}$=8.379 $^{kJ}/_{mol}$ with solubility product constant: $\mathbf{K_{sp}}_{CO2aqua}=[\mathbf{CO_{2aqua}}]/[\mathbf{CO_{2gas}}]/[\mathbf{H_2O}]$=EXP(-$\Delta\mathbf{G}_{spCO2aqua}$/R/T)=EXP(-8379/8.3144/298.15)=0.034045 and free energy increases about $\Delta\mathbf{G}_{spCO2aqua}=\mathbf{-R•T•ln(K_{sp}}_{CO2aqua})$=-8.3144*298.15*ln(0.034045)/1000=8.379 $^{kJ}/_{mol}$.

The reaction $\mathbf{CO_{2aqua}}+2\mathbf{H_2O}+\mathbf{\Delta G}+\mathbf{Q}=\mathbf{v1}\xrightarrow{CA}\mathbf{H_3O^+}+\mathbf{HCO_3^-}$ velocity constant is $\mathbf{k_1}_{CO2aqua}=1.5\times10^8$ $M^{-1}s^{-1}$ and acid equilibrium constant $\frac{[HCO_3^-]_{aqua}\cdot[H_3O^+]}{[CO_2]_{aqua}\cdot[H_2O]^2}=\mathbf{K_{eq}}_{CAHCO3aqua}=\mathbf{K_{a\_CO2aqua}}/[\mathbf{H_2O}]^2=10^{-7.0512}/55.3^2=2.906*10^{-11}$.[9]

CA high rate protolysis constant accumulate free energy for products $\mathbf{H_3O^+}$+$\mathbf{HCO_3^-}$ activate its.[1,8,14] $\Delta G_{eqCO2aqua}$=-**R•T•ln**($K_{eqCO2aqua}$)=-8.3144*298.15*ln(2.906*10^(-11))/1000=60.14 $^{kJ}/_{mol}$. The total free energy is activated to$G_{H3O+HCO3}$=G_{H3O+}+G_{HCO3-}=22.44+46.08=$\Delta G_{spCO2aqua}$+$\Delta G_{eqCO2aqua}$=8.379+60.14=68.52 $^{kJ}/_{mol}$

3) Water free energy content according Alberty increases from zero to $G_{H2O\_Biochemistry}$=**85.**64 $^{kJ}/_{mol}$. [1,8] Distilled water zero level $\mathbf{H_2O}_{distilled}$ $\xrightarrow{activation}$ $\mathbf{H_2O}_{Biochemistry}$ biochemically activates to **85.**64 $^{kJ}/_{mol}$ value;

$G_{H2O\_Biochemistry}$=$\Delta G°_{H2O\_Biochemistry}$-$\Delta G°_{H2O\_distilled}$=**-151.549**-(-237.191)=**85.**64 $^{kJ}/_{mol}$. [1,8]

Endoergic free energy accumulation create Attractors in biochemical medium as osmolar concentration C_{osm}=0.305 M, ionic strength I=0.2 M, pH=7.36, CA and etc., which drive Self-Organization of irreversible Homeostasis. High rate protolysis Attractors create water $G_{H2O\_Biochemistry}$=**85.**64 $^{kJ}/_{mol}$ activated from zero G_{H2O}.

4) Activated reactants G_{H3O+}+G_{HCO3-}=22.44+46.08=68.52 $^{kJ}/_{mol}$ in Photosynthesis transfer free energy to products. Reaction 6$\mathbf{H_3O^+}$+6$\mathbf{HCO_3}$=>$\mathbf{C_6H_{12}O_6}$+6$\mathbf{O_2}_{aqua}$+6$\mathbf{H_2O}$ quasi state equilibrium accumulate free energy change: 2840 $^{kJ}/_{mol}$=$\mathbf{G_{C6H12O6}}$+**6***$G_{O2Homeostasis\_arterial}$+**6***$G_{H2O\_Biochem}$-(6*$G_{H3O+}$+6*$G_{HCO3-}$).Actual reactants generate free energy sum assigned to glucose $\mathbf{G_{C6H12O6}}$=2268.8 $^{kJ}/_{mol}$ one mole andto oxygen six moles 6*G_{O2aqua}=6*78.08= 468.48 $^{kJ}/_{mol}$ and else to six water moles 6*G_{H2O}=6***85.**64 =513.84 $^{kJ}/_{mol}$, to CA activated products 6*G_{H3O+}+6*G_{HCO3-}=6*68.52=411.12 $^{kJ}/_{mol}$. Photosynthesis generate glucose 6th page free energy $\mathbf{G_{C6H12O6}}$=2268.8 $^{kJ}/_{mol}$ and reduction potential $\mathbf{E°_{C6H12O6}}$=-0.495 Volts. Oxidation progress of ordered Homeostasis generate irreversible concentrations gradients **6**$\mathbf{HCO_3^-}$+**6**$\mathbf{H_3O^+}$ for transport down and for osmosis of 6$\mathbf{O_2}_{aqua}$+6$\mathbf{H_2O}$ against the gradients. Sum $\mathbf{G_{C6H12O6}}$+6*G_{O2aqua}+6*G_{H2O}=2268.8+468.48+513.84=3251 $^{kJ}/_{mol}$ glucose oxidation reactants to products sum are 6*G_{H3O+}+6*G_{HCO3-}=6*68.52=411.12 $^{kJ}/_{mol}$.

3251 $^{kJ}/_{mol}$ sum $\mathbf{C_6H_{12}O_6}$+6$\mathbf{O_2}_{aqua}$+6$\mathbf{H_2O}$=osmosis=>channels<=transport=6$\mathbf{H_3O^+}$+6$\mathbf{HCO_3}$sum 411 $^{kJ}/_{mol}$.[1,8]

5) Water protolysis increases free energy content from zero water level G_{2H2O}=0 $^{kJ}/_{mol}$ in to activate products accumulating free energy G_{H3O+OH}=G_{H3O+}+G_{OH-}=22.44+77.36=99.8 $^{kJ}/_{mol}$:

$$H_2O+H_2O<=>H_3O^+ + OH^-: \quad \frac{[OH^-]\cdot[H_3O^+]}{[H_2O]\cdot[H_2O]} = K_{H3O^+ + OH^-} = [OH^-]*[H_3O^+]/[H_2O]^2 = 3.26\bullet10^{-18},$$

$\Delta G_{H3O^+ + OH^-}$=-R•T•ln($K_{H3O^+ + OH^-}$)=-8.3144*298.15*ln(3.26•10^(-18))/1000=99.8 $^{kJ}/_{mol}$,

$G_{H3O^+ + OH^-}$=G_{H3O^+}+G_{OH^-}-2*G_{H2O}=22.44+77.36-2*0=-R•T•ln($K_{H3O^+ + OH^-}$)=99.8 $^{kJ}/_{mol}$. [1,8,14]

6) Peroxide **2**$\mathbf{H_2O_2}$ protolysis enable catalysis for life resources ω=6, $\mathbf{O_2}_{aqua}$+**2**$\mathbf{H_2O}$+**2**$\mathbf{H_2O}$+**Q**.

High rate protolysis elevate free energy of peroxide 364.8 $^{kJ}/_{mol}$to protolysis products H_3O^+ and anion of peroxide G_{H3O+}+G_{HOO-}=22.44+418.32=440.76 $^{kJ}/_{mol}$ on zero reference G_{H2O}=G_{CO2gas}=0 $^{kJ}/_{mol}$ scale.

1) Activity initiate protolysis , than 2) collision disproportionate **OO** atoms and 3) finally neutralizes.

1) High rate protolysis $\mathbf{HOOH+H_2O \Leftrightarrow H_3O^+ + HOO^-}$ pK_a=11.75 make possible 2) collisions of anions $\mathbf{HOO^-}$><$\mathbf{^-OOH}$ with high activation energy $\mathbf{E_a}$=79000 $^{J}/_{mol}$ and slow velocity constant $\vec{\mathbf{k}}$ =1.416*10^{-16} $M^{-2}s^{-1}$ 3) disproportionate $\mathbf{^-OOH}$ atoms exothermic and oxidize collided oxygen atoms about $\mathbf{O_2}_{aqua}$.

Non colliding oxygen atoms reduce about 2 $\mathbf{OH^-}$ ions, which neutralizes with hydroxonium to water:

$$\mathbf{2H_2O_2+2H_2O \rightarrow H_3O^+ + HOO^- >< {}^-OOH + H_3O^+ \rightarrow O_2}_{aqua}\mathbf{+2H_2O+2H_2O+Q}.$$

Catalase the ions negative to positive collision $\mathbf{HOO^-}$>$\mathbf{Fe^{3+}}$ have $\mathbf{E_a}$=29 $^{J}/_{mol}$ indispensible law activation energy with protonation at first **His74** on second Asn147 what velocity constant increases 30 million times:

$$\mathbf{H_2O_2+H_2O_2+Fe^{3+} \rightarrow His74\text{-}H^+ + HOO^- > Fe^{3+} < {}^{--}OOH} + \text{Asn147-}\mathbf{H^+ \rightarrow O_2}_{aqua}\mathbf{+H_2O+H_2O+Q}_{exothermic}\mathbf{+Fe^{3+}}.$$

$\vec{\mathbf{k}} = \mathbf{A}\bullet\mathbf{e}^{-\frac{Ea}{RT}}$ =0.131*$\mathbf{e}^{-\frac{29}{8,314\bullet298}}$ =0.131*0.988=0.1296 $M^{-2}s^{-1}$; $\sqrt[CAT]{\vec{\mathbf{k}}} / \sqrt{\vec{\mathbf{k}}} = \frac{0,36}{1,19\bullet10^{-8}}$ =30*10^6.

In summary Catalase produce the Life resources ω=6, $\mathbf{O_2}_{aqua}$+2$\mathbf{H_2O}$+2$\mathbf{H_2O}$+**Q**:

7) High rate protolysis Attractors Catalase reactivity is indispensable Brownian molecular engine driving perfect order reactions of irreversible Homeostasis progress with production the hundred percents 100% efficiency ω=6, 3 fatty acids and the life resources: **oxygen**+**water**+**heat** for evolution and for survival.

8) High rate protolysis Attractors pH=7.36, CA, $\mathbf{H_2O}$, Shuttle Hemoglobin functionally activate $\mathbf{O_2}$,$\mathbf{CO_2}$. For dominate primary Attractor of Biosphere the bicarbonate buffer of Brensted protolysis :

$$\mathbf{CO_2}_{aqua}\mathbf{+2H_2O} <=^{CA}> \mathbf{H_3O^+ + HCO_3^-}$$

Henderson Haselbalh expression calculates the primary Attractor value pH=7.36 for Human blood:

$$pH = pK_a + \log\frac{[HCO_3^-]}{[CO_2]_{aqua}} = 7.0512 + \log(0.0154\ M / 0.0076\ M) = 7.36.\ [14]$$

3. Hess zero standard values of **elements** actually are positive energies. G_{H2gas}=**85.**6 $^{kJ}/_{mol}$ by Alberty referring to Homeostasis products water and $\mathbf{CO_2}_{gas}$ zero G_{H2O}=G_{CO2gas}=0 $^{kJ}/_{mol}$. Some reactants [1,8] are:

Glucose $\mathbf{G_{C6H12O6}}$=2268.8 $^{kJ}/_{mol}$>Peroxide protolysis products G_{H3O+}+G_{HOO-}=22.44+418.32=441 $^{kJ}/_{mol}$> >Peroxide G_{H2O2}=365 $^{kJ}/_{mol}$>G_{O2aqua}=330 $^{kJ}/_{mol}$>Ammonium G_{NH4+}=324 $^{kJ}/_{mol}$>oxygen G_{O2gas}=303 $^{kJ}/_{mol}$> > G_{N2gas}=**107.2** $^{kJ}/_{mol}$> protolysis of Water pH=pOH=7 $G_{H3O+OH-}$=G_{H3O+}+G_{OH}=22.44+77.36=99.8 $^{kJ}/_{mol}$> >G_{H2gas}=**85.**6 $^{kJ}/_{mol}$=$G_{H2O\_Biochemistry}$=**85.**6 $^{kJ}/_{mol}$ Alberty [8] > $G_{O2Biochem\_arterial}$=78.1 $^{kJ}/_{mol}$ [$\mathbf{O_2}_{arterial}$]=6*10^{-5} M > >Carbonic Anhydrase generate products are $G_{H3O+HCO3}$=G_{H3O+}+G_{HCO3-}=22.44+46.08=68.5 $^{kJ}/_{mol}$> >metallic Hydrogen $\mathbf{G_{H(Pt)}}$=51 $^{kJ}/_{mol}$> $\mathbf{G_{(Pt)}}$=38,4 $^{kJ}/_{mol}$>Homeostasis products zero values G_{H2O}=G_{CO2gas}=0 $^{kJ}/_{mol}$> > rhombic Sulfur $G_{Srhombic}$=**-85.**64 $^{kJ}/_{mol}$>Hydrogen Sulfide aqua $G_{H2Saqua}$=-571 $^{kJ}/_{mol}$ in descending order.

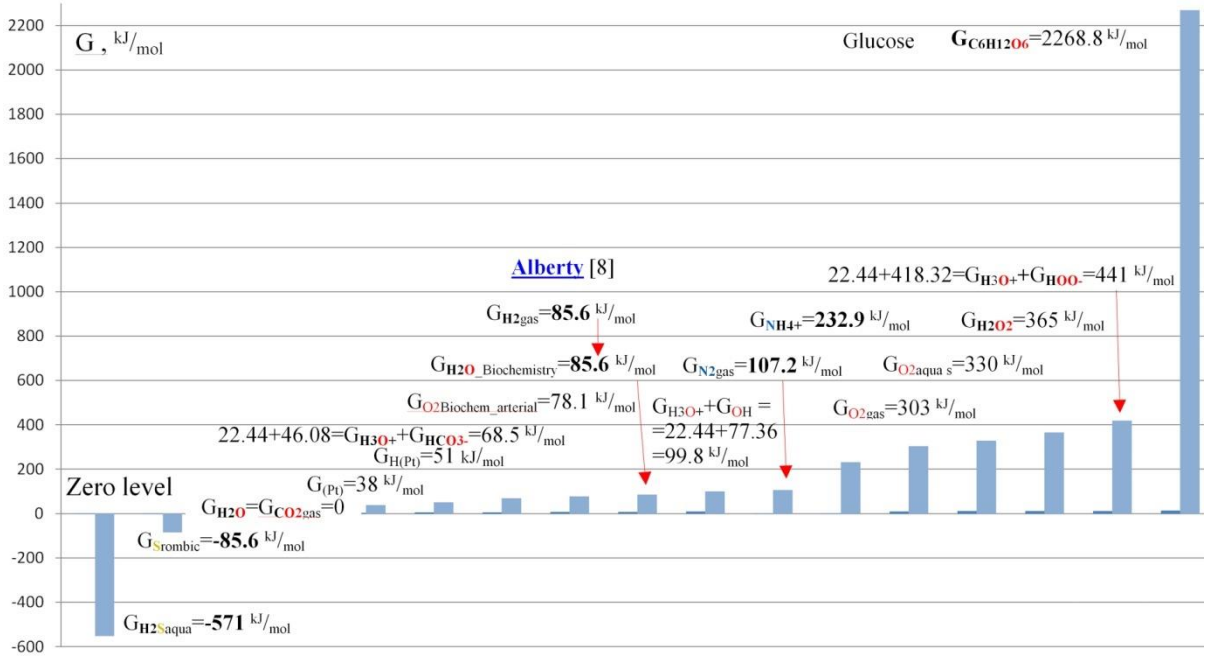

Fig. 1. Free energy content starting from zero $G_{H2O}=G_{CO2gas}=0$ kJ/mol of Homeostasis metabolites ascending.

Hydroxonium reduction by proton captures electron from platinum lattice H_3O^++(Pt)+e^-⇔(Pt)H+H_2O produce metallic (Pt)H. Hess is $\Delta G_{Hess}=G_{H2O}+G_{H(Pt)}-G_{H3O+}-G_{(Pt)}-G_{e-}$=22,44+**38,4**+0-(0+**51**)=9,765 kJ/mol. free energy change. The equilibrium $\Delta G_{eq}=E^{\circ}_{H}\bullet F\bullet 1\bullet 1$=0,1016*96485*1/1000= 9.81 kJ/mol shows free energy change positive of metallic Hydrogen (Pt)H reduction potential on zero scale $G_{H2O}=G_{CO2gas}=0$ kJ/mol of free electron, water and CO_{2gas} .High rate protolysis Attractors pH=7,36 and $[O_{2aqua}]=6*10^{-5}$ M activate metallic Hydrogen (Pt)H and Glucose $C_6H_{12}O_6$ to strong reduction potential -0,436 Volts 3rd page and -0,393 V:

$E_{(Pt)H=7,36}$=0,1016+0,0591*log($10^{-7,36}$/55,3)=-0,436 V and $E_{C6H12O6}=\Delta E+E_{O2}$=-1,226+0,833=-0.393 V.

4. O_{2aqua} Hemoglobin shuttle exchange with **metabolic** generate **HCO_3^-** and **H^+ gradients** across membranes.

Hemoglobin in tissue desorbs oxidant oxygen **O_{2aqua}** for exchange by oxidation products HCO_3^-, H^+ In lungs HCO_3^- and H^+ release due to adsorption of oxygen **O_{2aqua}**. [6] Exchange equilibrium affinity of hemoglobin to oxygen increases reaching mole fraction $[Hb_R(O_2)]$=0.96 concentration $[O_{2aqua}]=6*10^{-5}$ M in arterial blood and deoxy mole fraction lefts $[(H^+BPG^{5-})Hb_T$...salt bridge...$(HCO_3^-)]$=0.04.In tissue Bisphospho glycerate **BPG^{5-}**of erythrocyte squeezed in hemoglobin creates deoxy mole fraction 0.37=$[(H^+ BPG^{5-})Hb_T$...salt bridge...$(HCO_3^-)]$ and decreases oxy to $[Hb_R(O_2)]$=0.63 mole fraction. In circulation organism consume 0.37-0.04=0.33 oxygen mole fraction sustaining venous $[O_{2aqua}]=0.426\cdot10^{-5}$ M concentration. $[HCO_3^-]/[CO_{2aqua}]$=0.0154 M/0.0076 M ratio stabilizing at pH=7.36 level as multi-functional Attractor of Self-Organization. Actual seven components concentrations at saturated oxygen arterial blood and consumed 0.33 oxygen venous state:

$$O_2+(H^+BPG^{5-})Hb_T\ldots\text{salt-bridge}\ldots(HCO_3^-)+H_2O\leftrightarrow Hb_R(O_2)+H_3O^++HCO_3^-+BPG^{5-};[6,14]$$

$K=[Hb_R(O_2)]*[BPG^{5-}]*[H_3O^+]*[HCO_3^-]/[(H^+BPG^{5-})Hb_T$..salt bridge...$(HCO_3^-)]/[H_2O]$ /$[O_{2aqua}]=2.43*10^{-8}$;
$K=[Hb_R(O_2)]*[BPG^{5-}]*[H_3O^+]*[HCO_3^-]$ /$[Hb_T]$ /$[H_2O]$ /$[O_{2aqua}]=2.43*10^{-8}$;
arterial blood $K=0.96*\mathbf{0.005}*10^{-7.36}*0.0154/0.04$ /55.3 /$6/10^{-5}=2.43*10^{-8}$;
venous blood $K=0.63*\mathbf{0.005}*10^{-7.36}*0.0154/0.37$ /55.3 /$0.426/10^{-5}=2.43*10^{-8}$;
high land
venous blood $K=0.48*\mathbf{0.008}*10^{-7.36}*0.0154/0.52$ /55.3 /$0.3692/10^{-5}=2.43*10^{-8}$;

See level air Attractor $[O_2]$=20.95% make in erythrocytes $[BPG^{5-}]$=**5 mM**, but high land (see Oxygen in blood [6] low air $[O_2]$ in erythrocytes have content of $[BPG^{5-}]$=**8 mM** and keep equilibrium at $K=2.43*10^{-8}$.

Stabilized multi functional Attractor pH=7.36 keep $[HCO_3^-]$=0.0154 M, $[CO_{2aqua}]$=0.0076 M despite blood circulation cycle generate amounts of $[H^+]=459*6\bullet10^{-5}$ M and 0.0275 M=$[HCO_3^-]$. Arterial concentrations $[O_2]=6\cdot10^{-5}$ M, $[Hb_R(O_2)]$=0.96, $[(H^+)Hb_T$..salt bridge..$(HCO_3^-)]$=0.04 and venous Homeostasis concentrations are $[O_2]=0.426\cdot10^{-5}$ M, $[Hb_R(O_2)]$=0.63, $[(H^+)Hb_T$...salt bridge...$(HCO_3^-)]$=0.37.[6,14]

Self-Organization Attractors pH=7.36, CA Carbonic Anhydrase, water **H_2O** create functional activity with charged groups negative and positive: **HPO_4^{2-}**, **HCO_3^-**, **R-COO^-**, **R-NH_3^+**, **R-PO_4^{2-}**now free now linked in molecules **R**: amino acids, proteins, nucleic acids, carbohydrates, coenzymes. BUFFERs 11th, 12th pages:. [1]

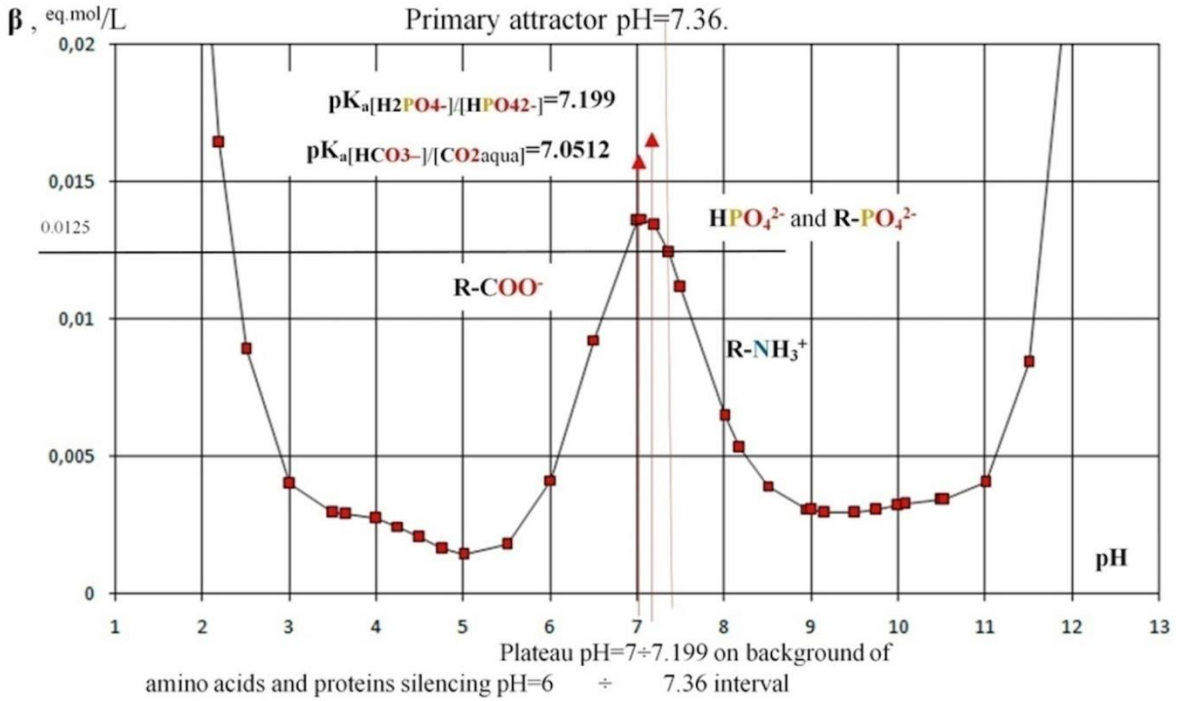

Fig. 2. Bicarbonate alkaline reserve ratio 2/1=[$\mathbf{HCO_3^-}$]/[$\mathbf{CO_{2aqua}}$] and phosphates [$\mathbf{H_2PO_4^-}$]/[$\mathbf{HPO_4^{2-}}$]=1,45/1 alkaline reserve ratio on background of proteins silencing interval from pH=6 to pH=7,36. The three buffer systems create broad band buffer capacity **β** maximum plateau on interval from pH=7 to pH=7,199. [14]

In blood *plasma* dominate two buffers: the enzyme **CA** Carbonic Anhydrase bicarbonate and phosphate buffer with capacity maximums plateau interval pH 7÷7.199. Alkaline reserve 2 and 1.45 at Attractor **pH=7.36** value is created on the protein buffer capacity silencing interval from pH=6 to pH=7.36 background. BUFFERs
Also in cytosols, sweat, urine and digestive apparatus dominate bicarbonate and phosphates common buffer.

High rate protolysis Attractors **pH**=7.36, CA, $\mathbf{H_2O}$ functionally activate arterial and venous oxygen concentrations by driving oxygen $\mathbf{O_2}$ Shuttle Hemoglobin to exchange of bicarbonate $\mathbf{HCO_3^-}$ and proton H^+ for transport in blood circulation from lungs to tissues and reverse $\mathbf{HCO_3^-}$, H^+ to $\mathbf{O_2}$. Those exchange on interface to environment through Homeostasis irreversible reactions in ***lungs*** from AIR inhaling $\mathbf{O_2}$ and exhaling $\mathbf{CO_2}$. High rate protolysis Attractors activate in perfect order Brownian molecular engines and creates Self-Organization the biosphere for irreversible Homeostasis to evolution and survival.

5. Results and Conclusions Summary.

Attractor studies reveal thermodynamics standard potential for metallic Hydrogen incorporate in platinum lattice: $H_3O^+ + (Pt) + e^- \Leftrightarrow (Pt)H + H_2O$ at standard mole fractions the logarithm of $\mathbf{K_{eq}}=X_{H3O+}/X_{H2O}=1$ is zero and

potential is $\mathbf{E}=E^\circ_H + \frac{\ln(10)\bullet R\bullet T}{F\bullet 1}\bullet\log\frac{X_{H_3O^+}}{X_{H_2O}} = E^\circ_H+0=$ 0.10166 Volts over classic zero $E^\circ_{Hclassic}=0$ V. [1]

Hydrogen metal reduction half reaction shows $\mathbf{G_H}=E^\circ_H\bullet F\bullet 1\bullet 1=0.10166*96485*1/1000=$ 9.81 $^{kJ}/_{mol}$ free energy positive. Hess give $\Delta\mathbf{G}_{Hess}=G_{H2O}+G_{H(Pt)}-G_{H3O+}-(G_{(Pt)}+G_{e-})=22{,}44+\mathbf{38{,}4}+0-(0+\mathbf{51})=$ 9,765 $^{kJ}/_{mol}$ on [8].

High rate protolysis Attractors pH=7,36 and $[O_{2aqua}]=6*10^{-5}$ M activate metallic Hydrogen (Pt)H and Glucose $\mathbf{C_6H_{12}O_6}$ to strong reduction potential -0,436 Volts 3rd page and -0,393 Volts:

Reference scale has based on Alberty Hydrogen $G_{H2gas}=\mathbf{85.6}$ $^{kJ}/_{mol}$, in water $G_{H2aqua}=\mathbf{103}$ $^{kJ}/_{mol}$, and metallic hydrogen $\mathbf{G}_{H(Pt)}=51$ $^{kJ}/_{mol}$ referring to Homeostasis zero $G_{e-}=G_{H2O}=G_{CO2gas}=0$ $^{kJ}/_{mol}$ value of free energy which belongs to free electrons e^-, for water $\mathbf{H_2O}$ and $\mathbf{CO_{2gas}}$. [8]

- The oxygen $\mathbf{O_{2aqua}}$ molecules make functional activation as fire safe Biochemistry in water solution with protolytic decreasing free energy content from $G_{O2aqua}=330$ $^{kJ}/_{mol}$ to blood $G_{O2Homeostasis\_arterial}=78.08$ $^{kJ}/_{mol}$.
- Carbonic Anhydrase CA enzyme governed carbon dioxide protolysis increase free energy content of products $\mathbf{H_3O^+}+\mathbf{HCO_3^-}$ from zero $\mathbf{CO_{2gas}}+2\mathbf{H_2O}$ to $G_{H3O+}+G_{HCO3-}=22.4+46.1=68.5$ $^{kJ}/_{mol}$.
- Water in biochemical medium increases free energy to $G_{H2O\_Biochemistry}=\mathbf{85.65}$ $^{kJ}/_{mol}$. [1,8,14]
- Photosynthesis (6th page) of glucose free energy $\mathbf{G}_{C6H12O6}=2268.8$ $^{kJ}/_{mol}$ generate concentrations gradients $6HCO_3^- + 6H_3O^+$ free energy of $6G_{H3O+}+6G_{HCO3-}=411$ $^{kJ}/_{mol}$ across membranes for transport and osmosis reverse.
- Water protolysis increases free energy from zero $2*G_{H2O}=0$ $^{kJ}/_{mol}$ to $G_{H3O+}+G_{OH-}=22.4+77.4=99.8$ $^{kJ}/_{mol}$.
- Catalase with high rate protolysis increase peroxide molecules activity from $\mathbf{E_a}=79000$ $^{J}/_{mol}$ to $\mathbf{E_a}=29$ $^{J}/_{mol}$.

● High rate protolysis Attractors created Catalase reactivity $30*10^6$ times greater velocity constant which is indispensable Brownian molecular engine for essential ω=6, ω=3 fatty acids elongation in peroxisomes.

● High rate protolysis functionally activate revised molecules on behalf of rule Attractors including CA Carbonic Anhydrase synthesis, which stay at equilibrium as **pH**=7.36, as water concentration [$\mathbf{H_2O}$]=55.3 M, as oxygen concentration [$\mathbf{O_2}$]=20.95 % on air during 500 MYears, as arterial [$\mathbf{O_{2aqua}}$]=$6*10^{-5}$ M and [$\mathbf{O_{2aqua}}$]=$0.426*10^{-5}$ M venous oxygen concentration, which are indispensable for isooxia in bioenergetic and irreversible progress of Homeostasis. [14]

The order of functionally active molecules drive irreversible Homeostasis under rule Attractors, which stay at equilibrium, while Homeostasis continues with $\mathbf{CO_2}+2\mathbf{H_2O}$ protolysis generate indispensable concentrations $\mathbf{H_3O^+}+\mathbf{HCO_3^-}$ gradients of free energy $G_{spCO2}+G_{CA}$=8,38 $^{kJ}/_{mol}$+60 $^{kJ}/_{mol}$. Using the gradients energy Brownian molecular engines drive irreversible homeostasis of $\mathbf{H_3O^+}+\mathbf{HCO_3}$ for transport down the gradient through membrane cannels exhaling $\mathbf{CO_{2gas}}+\mathbf{H_2O}$ and inhaling $\mathbf{O_{2aqua}}+\mathbf{H_2O}$ for osmosis against the gradients through aquaporins. Photosynthesis with carbonic anhydrase CA inhale $\mathbf{CO_{2gas}}+\mathbf{H_2O}$ through proton $\mathbf{H^+}+\mathbf{HCO_3}$ bicarbonate cannels and exhale $\mathbf{O_{2aqua}}+\mathbf{H_2O}$ through aquaporins cannels in osmosis manner establish global Attractor oxygen [$\mathbf{O_2}$]=20.95%. Reaching the Attractor values create the perfect order of Homeostasis out of disorder, out of chaos. Deviation from Attractors values disorder the Homeostasis and brings to the chaos that cause loss the Homeostasis order of functional activity. [5] Chaotic disordered reactions waste the resources and stop the Homeostasis, stop the progress of perfect order non-equilibrium complex processes. The Homeostasis becomes extinct from Biosphere.

The irreversible Homeostasis by Attractors ordered five type enzymatic composite **reactants** and **products** as Self-Organization trends to reach **equilibrium** state, but never reaches as Homeostasis are perfect ordered non equilibrium states. The Nobel Prize in Chemistry 1977th . [4,5]

Attractors are two types and multipurpose. The primary Attractors are common for Biosphere. The secondary Attractors are for individual organisms. The multipurpose Attractors are both primary and secondary. The primary global Attractors are multipurpose pH=7.36, water [$\mathbf{H_2O}$]=55.3 M and oxygen [$\mathbf{O_2}$]=20.95% inair during 500 MYears. [14]

6. Acknowledgements.

The author would like to acknowledge all the contributions of the field “the Thermodynamic high rate protolysis Attractors functionally activate oxygen $\mathbf{O_2}$, carbon dioxide $\mathbf{CO_2}$ ” which critically appreciate this study:

Thanks for critical discussions with MD Aivar Grinberg about Attractors in Biochemistry to see indispensability for Life create functionally activate molecules to maintain the irreversible Homeostasis.

Thanks for Riga Stradin’s University Library about supporting literature studies.

Thanks for Riga Stradin’s University department stuff of Human Physiology and Biochemistry who supporting my advanced studies in Biochemistry of Thermodynamic Attractors.

7.References.

[1]David R. Lide. CRC Handbook of Chemistry and Physics .90th ed. Taylor and Francis Group LLC; 2010 .
[2] Prigogine I., Defey R. Chemical Thermodynamics. Longmans Green & co ©; 1954.
[3] Prigogine I., Nicolis G. Self-Organization in Non-Equilibrium Systems. Wiley, 1977.
[4]Prigogine I. Time, Structure and Fluctuations. Lecture, The Nobel Praise in Chemistry; 1977.
[5]Kuman M. New light on the attractors creating order out of the chaos. Int J Complement Alt Med.; 2018; 11(6); 337.;
[6]Nelson DL, Cox MM. Lehninger Principles of Biochemistry. 5th ed. New York: W.H. Freman and company; 2008.
[7]Xing W, Yin G, Zhang J. Rotating Electrode Method and Oxygen Reduction Electrocatalysts. *Elsevier*; 6 (2014) .
[8]Alberty RA. Biochemical Thermodynamic's : Applications of Mathematics. John Wiley & Sons, Inc. 1-463, (2006).
[9]Pinard MA, Mahon B, McKenna R. Probing the Surface of Human Carbonic Anhydrase for Clues towards the Design of Isoform Specific Inhibitors. *BioMed Research International*; **2015**, 3 (2015).
[10]Kotz JC, Purcell KF. Chemistry and chemical reactivity. Saunders College Publishing; 1991.
[11]White VM. THE CARBON CYCLE, ISOTOPES, AND CLIMATE I and II. Lectures 37, 38; 2003 .
[12]Hanania J, Pomerantz C, Stenhouse K, Toor J, Donev J. Carbon cycle. University of Calgary's 2020 .
[13]Der wohltemperierte Planet. *Der Spiegel*. 2007 Nr.19:148-154. German .
[14] Kaksis A. The Biosphere Self-Organization Attractors drive perfect order homeostasis reactions to link bioenergetic with functionally activate oxygen and carbon dioxide molecules. 7th International Conference on New Trends in Chemistry September 25-26, 2021.27-32.

DNA BINDING STUDIES FOR SOME SMALL MOLECULES

Ayşegül GÖLCÜ

Department of Chemistry, Faculty of Arts and Sciences, Istanbul Technical University, Maslak, Istanbul 34469, Turkey.
e-mail:aysgolcu@itu.edu.tr

Abstract

DNA is the pharmacological target for many drugs in clinical use and further clinical trials. Because DNA is the executive molecule of the cell, it directs all life activities such as nutrition, respiration, and reproduction. It also regulates cell functions through DNA transcription (RNA synthesis) and copies itself (replication) during preparations for cell division. When the drug interacts with DNA, it either artificially alters or inhibits the functions of DNA. The drug's process of altering and inhibiting the function of DNA is very important for the control and treatment of the disease. In this study, the interaction mechanism of some small molecules such as newly synthesized ligand molecules, plant extract, and its derivatives, and some drug molecules, with double-stranded DNA was investigated by analytical (spectrophotometric and voltammetric) techniques. In addition, the binding constants (K_b) of each small molecule showing the ability to bind to DNA were compared with those in the commercial and literature.

Key Words: *DNA, binding mechanisms, ligand, plant extract, drug, spectroscopy, voltammetry*

1. Introduction

The mechanism of binding a small molecule with DNA has been studied for nearly fifty years[1]. DNA is a nucleic acid that carries the necessary information for all organisms and viruses to perform their vital functions and biological processes[2]. In 1953, researchers named Francis Crick and James Watson proposed the molecular structure of DNA and reported that this structure was a double helix structure. Accordingly, the DNA molecule consists of two spirally coiled strands, and these strands form the backbone of DNA. These strands make DNA look like a twisted ladder[2]. The edges of the stairs are composed of sugar (deoxyribose) and phosphate structures. Deoxyribose and phosphate structures, on the other hand, are linked to each other by phosphodiester bonds (the bond between one phosphate molecule and two sugar molecules). DNA is made up of many nucleotides. Each nucleotide contains an aromatic base (purine or pyrimidine), deoxyribose sugar (D), and a phosphate group. Sugar and phosphate groups in all nucleotides of DNA is the same. Nucleotides are named according to the bases they contain. These bases are divided into purine and pyrimidine bases. The purine bases are adenine and guanine; The pyrimidine bases are cytosine and thymine. In addition, bases and sugars are linked by glycosidic bonds[2]. The double chain in the helical structure of DNA is held together by hydrogen bonds between the bases. The adenine (A) and thymine (T) bases are linked by two hydrogen bonds, and the guanine (G) and cytosine (S) bases are linked by three hydrogen bonds. In the double-chain helix, these bases are hydrophobic because they are located inside the helix, and hydrophilic because there is a sugar and phosphate backbone on the outside of the helix[5]. The distance where the DNA strands are closest to each other is called the small groove, and the distance where they are farthest from each other is called the big groove. Interacting molecules enter these large and small grooves of the DNA chain and form hydrogen bonds and Van der Waals bonds with DNA[2].

When any small molecule interacts with DNA, it either artificially alters or inhibits the functions of DNA. If this small molecule is a drug, this type of interaction is very important for the control and treatment of a disease, as it will cause the process of altering and inhibiting the function of DNA[3]. The intracellular target of antibiotics and anticancer drugs, which have a wide range of uses, is DNA[4]. Recently available against many malignant tumors Examining the drug and DNA interaction is important to treat the disease because of both the inadequacy of the treatments and their side effects. For this reason, the synthesis of new molecules aimed at recognizing the DNA-oriented structure directly in living cells is designed in both academia and industry in research laboratories[5]. The study of small molecules with pharmacological importance, especially drug molecules and DNA interaction, is one of the most important factors that play a role both in understanding the mechanism of interaction and in the design of new DNA-targeted drugs and the development of related processes[10]. Therefore, in this study, the interaction of some newly synthesized small molecules and drug molecules with double-stranded DNA was investigated spectroscopically and voltametrically. We applied a variety of spectroscopic methods under physiological situations, including UV-vis and fluorescence spectroscopy and thermal denaturation, and electrochemical measurements, as well as molecular docking investigations.

2. Experimental section

2.1. Reagents and materials

The dsDNA, tris(hydroxymethyl)aminomethane hydrochloride (Tris-HCl), NaCl, Ethidium Bromide (EtBr), Hoechst 33258, and Rhodamine B were purchased from Sigma-Aldrich Co. All solvents were purchased from

Merck and used without further purification. The dsDNA stock solution was prepared via the dilution of dsDNA with the buffer solution (containing 0.2 M Tris-HCI and 150 mM NaCl at pH 7.4) and kept at 4°C and consumed in a week. The dsDNA solution's UV absorbance ratio at 260 and 280 nm (A260/A280) proved that the dsDNA was sufficiently purified from protein contamination. The molar concentration of dsDNA was determined using the molar absorption coefficient, ε of 6600 $M^{-1}cm^{-1}$. For electrochemical analyses, dsDNA stock solution was prepared by diluting dsDNA with the acetate buffer solution with a pH of 4.8. All the aqueous solutions of Ethidium Bromide (EtBr), Rhodamine B, Hoechst 33258, and small molecule (1×10^{-3} M) were prepared in pure water (or DMSO).

2.2. Physical Measurements and Instrumentation

The absorption spectra were recorded in the range of 200–350 nm in a T80 + UV/VIS spectrophotometer, using the 1 cm light path cells. The denaturation profile of dsDNA solution (120 μM) was obtained by increasing the temperature from 10°C to 100°C while recording the absorbance values at 260 nm wavelength. Fluorescence measurements were performed in Agilent Technologies Spectrofluorometer using a quartz cell of 1 cm light path by keeping the concentrations of EtBr (Rhodamine B and/or Hoechst 33258) and dsDNA solutions constant at 5 μM, 50 μM, respectively. The electrochemical measurements were recorded with an Autolab potentiostat/galvanostat (PGSTAT 204, Eco Chemie, Netherlands). The experimental conditions were managed with GPES (General Purpose Electrochemical System) and Nova 2.2 software packages. Glassy carbon electrode (BAS; U: 3 mm diameter) was used in voltammetry studies, and all measurements were made using BAS 100 W (BioanalyticalSystem, USA) potentiometer. An Ag/AgCl reference electrode (BAS; 3 M KCI in all experiments), a platinum wire counter electrode, and a 10 ml standard single compartment three-electrode cell were used for the triple electrode system. Before each measurement, the glassy carbon electrode surface is manually polished and cleaned with a slurry of alumina powder (U: 0.01 cm) with regular circular motions on a specific suede soft polishing cloth (BAS suede polishing pad). All binding experiments were conducted in triplicate and relative standard deviations (RSD) from the mean in the calculated binding constants were determined for all techniques.

2. Results and discussion

While DNA-targeted design of many newly synthesized substances with pharmacological properties is carried out, it is extremely important for science to clarify the interactions of these substances with DNA quickly and effectively. This lighting will enable these studies to progress more rapidly in line with their purpose. Small molecules can bind to DNA by two basic interactions: covalent or non-covalent bonding (electrostatic, intercalation, and slotting).[7] For small molecules to interact covalently with DNA, they must have ligands that can hydrolyze when taken into the labile cell, such as chloride in cisplatin[8]. In addition to cis-platinum and other platinum compounds, nitrogen mustard drugs such as melphalan, uramustine, chlorambucil and bendamustine, other small molecule species of pharmacological importance such as Mitomycin C and Psoralen have been found to covalently bind DNA[9]. Non-covalent bonding forms are divided into four classes among themselves: (i) electrostatic interaction with the anionic sugar-phosphate backbone of DNA, (ii) penetrating into major or minor grooves of DNA, (iii) intercalation between base pairs of DNA, (iv) screw intercalation (covalent bonding + intercalation or bonding to grooves + intercalation)[6]. In the last two decades, we have used UV–vis absorption spectra and fluorescence spectrophotometric methods, which are spectrophotometric methods, to determine the binding mechanism and binding constants.

2.1. UV–vis absorption spectra methods

The examination of UV–vis absorption spectra is one of the most basic methods used in the interaction of complexes with DNA. In these studies, UV-vis absorption spectra of the solutions prepared by adding increasing amounts of DNA while keeping the small molecule concentration constant were recorded. UV–vis spectra of small molecule−DNA solutions were scanned in the wavelength range of 200 to 400 nm. Changes in the absorption bands observed at this wavelength were followed. As a result of the interaction of small molecules with DNA, changes occur in the helical structure of DNA. The decrease in the absorption band with increasing DNA concentration indicates the hypochromic effect, and the increase indicates the hyperchromic effect. The decrease in the absorption band with increasing DNA concentration indicates the hypochromic effect, and the increase indicates the hyperchromic effect. The hypochromic effect causes shrinkage or shortening of the DNA along the helical axis, while the hyperchromic effect causes bending in the helical structure of the DNA. In some cases, the small molecule causes a red or blue shift in the absorption band of DNA as well as a hyper- or hypochromic effect. In addition to the hyperchromic effect in the absorption spectra, the redshift shows the stability of the new complex-DNA structure. In the UV spectra of small molecule−DNA solutions, the upward

arrow indicates the increase in absorption due to increasing DNA concentration, and the downward arrow indicates the decrease in absorption (Fig. 1a and b)[10,11].

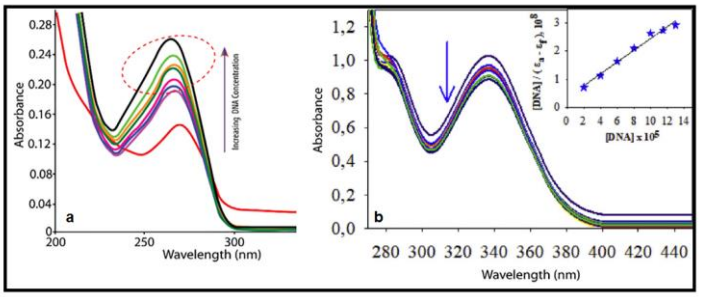

Fig. 1. Increase (a) and decrease (b) in absorption due to increasing DNA concentration in UV spectra of small molecule-DNA solutions

Based on the UV-Vis absorption spectra, the binding constants (Kb) of small molecules with double-stranded DNA were determined using the equation (Eq. 1) below12.

$$\frac{[\text{dsDNA}]}{\varepsilon_a - \varepsilon_f} = \frac{[\text{dsDNA}]}{\varepsilon_b - \varepsilon_f} + \frac{1}{k_b(\varepsilon_b - \varepsilon_f)} \qquad \text{(Eq. 1)}$$

Where εa is the apparent extinction coefficient calculated using Aobsd/[small molecule], and εf is the molar extinction coefficient of the small molecule-free form that hasn't interacted with dsDNA. εb is the molar extinction coefficient of the completely interacted small molecule with dsDNA, and [dsDNA] is the concentration of dsDNA in terms of base pairs.

Some Kb values calculated using this formula within the scope of our studies are given in Table 1.

Table 1. K_b values obtained by UV-Vis absorption titration

Small Molecule Name	Chemical Structure of Small Molecule	Media	K_b	Reference
Trimethoprim	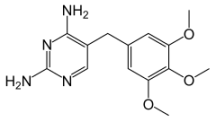	Buffer solution containing 150 mM NaCl and 15 mM Tris–HCl	5×10^4	13
Trimethoprim-copper complex	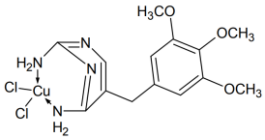	Buffer solution containing 150 mM NaCl and 15 mM Tris–HCl	66×10^7	13
Valaciclovir	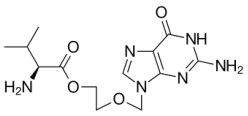	Buffer solution containing 150 mM NaCl and 15 mM Tris–HCl	0×10^4	14
Ofloxacin	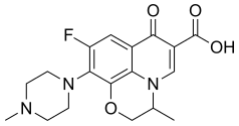	Buffer solution containing 150 mM NaCl and 15 mM Tris–HCl	2×10^4	15

2.2. Fluorescence Spectroscopy Method

The basis of this method is the displacement studies with Ethidium bromide (EB), Hoechst 33258, and Rhodamine B using fluorescence spectroscopy. EB is a planar molecule and is intercalated between dsDNA base pairs, while Hoechst 33258 is a molecule that can enter the small grooves of dsDNA. While these molecules show weak fluorescence alone, their emission intensities increase significantly when bound to DNA. Figures a show the reductions caused by small molecules in EB-DNA solutions (Rhodamine B -DNA solutions in Figure 2 b)16.

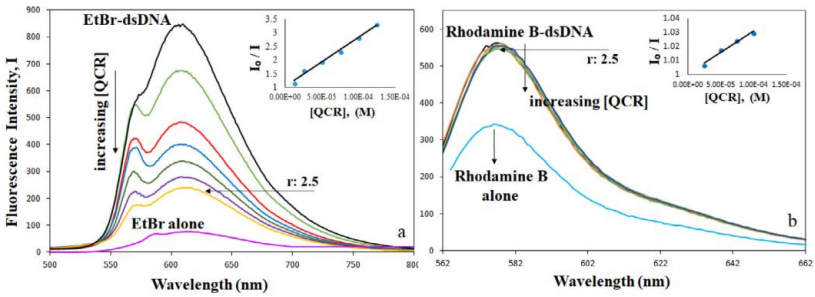

Fig. 2. Fluorescence titration of a) EtBr-dsDNA, b) Rhodamine B-dsDNA mixtures with quercetin. a) and b) insets: Stern-Volmer plots; they show the fluorescence quenching of a) EtBr-dsDNA complex b) Rhodamine B-dsDNA complex by the increasing addition of quercetin. The r values on the graphs show the ratios of [quercetin]/[dsDNA].

Stern-Volmer constant (K_{SV}) values of the fluorescence quenching abilities of small molecules are calculated[17].

$F_0/F = 1 + K_{SV}$ [small molecule]

While F_0 indicates the emission intensities of only EB-DNA solution and F of EB-DNA solutions in the presence of complex, K_{SV} is called extinction coefficient. In such studies, the Stern-Volmer plots shown in Figure 2 a and b are obtained by using fluorescence data. K_{SV} values of small molecules calculated from the slopes of the lines in the graphs are calculated. The K_{sv} values of EtBr and Rhodamine B bound dsDNA complexes were calculated to be 1.82×10^4 M^{-1} and 4.23×10^2 M^{-1}, respectively. Higher K_{sv} shows that EtBr replacement by quercetin exists compared to Rhodamine B.

2.3. Cyclic Voltammetric Technique

Cyclic voltammetry technique is one of the important methods used in the study of electrochemical events. With this technique, current is measured as a function of voltage. The alternating voltammogram is obtained by plotting the change in current in a certain range against the constantly changing potential values. In the method, the current response of the electrode in an unstirred solution is excited by a triangular wave potential. The interaction of any small molecule with dsDNA can be successfully detected by the alternating voltammetry technique. This detection can be achieved through the guanine/adenine signal, which are the electroactive bases of dsDNA, or via the electrochemical signal of the small molecule to be analyzed. According to the changes in these signals, interpretations can be made about DNA–small molecule interactions[18]. Two ways are followed when examining the small molecule-dsDNA interaction with the revolving voltammetry technique. Two ways are followed when examining the small molecule-dsDNA interaction with the revolving voltammetry technique. The first of these is the change in the existing small molecule signal before and after the interaction, and the second is the change in the signal of the electroactive bases guanine and adenine in dsDNA, and according to this change, the interaction is interpreted[18]. In Fig.3, voltamagroms of the alternating voltammetry technique are given for both cases[19].

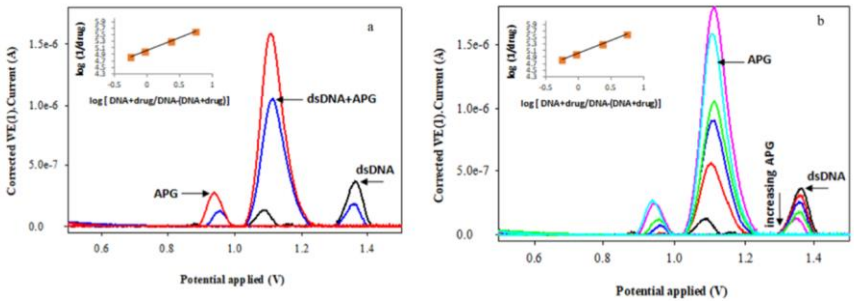

Fig. 3. Interaction of the molecule of Apigenin (APG) with dsDNA. (a) Cyclic voltammograms of dsDNA (black), Apigenin (red), and dsDNA incubated with APG (blue) in pH 4.8 acetate buffer. Cyclic voltammograms of 50 µM dsDNA (black) with increasing amounts of APG in pH 4.8 acetate buffer (b). The arrow shows the decreases in peak current with respect to increases in APG concentration.

In the cyclic voltammetry technique, the binding constant (Kb) is calculated using the formula[20] below:

$$\log(1/[\text{dsDNA}]) = \log K_b + \log[S_{\text{compound-dsDNA}}/S_{\text{compound}} - (S_{\text{compound-dsDNA}})]$$

The terms used in the equation are as follows: [dsDNA], dsDNA concentration alone; Scompound−dsDNA, current signal received from the compound after the interaction with dsDNA; and Scompound, current signal received from the compound alone. The Kb and log Kb values were calculated for each compound using this equation at room temperature. For example, according to the voltammograms' above, the Kb value for apigenin was found to be 1.05×105. This value agrees with the data obtained from spectrophotometric methods[19].

Conclusion

The interaction of small molecules with dsDNA and the elucidation of the mechanisms of these interactions are extremely important today. Recent advances in the structure-based design of small molecules targeting specific DNA sequences show that the promise of this field as a source of new therapeutic agents is beginning to come true. The interactions of small molecules synthesized and characterized in chemistry laboratories with dsDNA (and elucidation of interaction mechanisms) will contribute to the country's economy as well as being evaluated as new drug candidate molecules.

Acknowledgments

This work is supported by the Istanbul Technical University (Scientific Research Projects Unit) under TDA-2021-43309 project.

References

[1] Farias, S.T., Furtado, A. N. M., Junior, A. P. S., José, M.V., 2023, Natural History of DNA-Dependent DNA Polymerases: Multiple Pathways to the Origins of DNA, Viruses, 15(3), 749.
[2] Blackburn, G.M., Gait, M.J. 1990. Nucleic Acids in Chemistry and Biology, Oxford University Press, New York.
[3] Berman, H.M., Young, P.R., 1981, The interaction of intercalating drugs with nucleic acids, Annu. Rev. Biophys. Bioeng., 10, 87–114.
[4] DeRuiter, J., 2004, Principles of Drug Action 2, Fall.
[5] Delgado, J.N., Remers, W.A., Lippincott, J.B., 1991, Wilson and Gisvold's Textbook of Organic Medicinal Pharmaceutical Chemistry, 9th. ed: Williams, L. & Philadelphia, W., Pp: 39.
[6] Arnott, S., 1986, Major groove or minor groove?, Nature, 320, 313.
[7] Rosenberg, B., Van Camp, L., Grimley, E.B., Thomson, A.J., 1967., Inhibition of Growth or Cell Division in Escherichia Coli by Different Ionic Species of Platinium Complexes, Journal of Biological Chemistry, 242(6), 1347–1350.
[8] Lutz W.K., In vivo covalent binding of organic chemicals to DNA as a quantitative indicator in the process of chemical carcinogenesis., 1979, Mutat Res. 65(4), 289-356.
[9] Bolt, H.M., Laib, R.J., 1980, Covalent binding of drug metabolites to DNA--a tool of predictive value? Arch Toxicol , 46(1-2), 171-80.
[10] Güngör, Ö., Demircioğlu, Z., Gölcü, A, 2022, The new dimeric copper(II) complex from anticancer drug cytosine arabinoside, Journal of Molecular Structurethis link is disabled, 1270, 133826.
[11] Beyazit, N., Kaya, K., Şenel, P., Özdemir, A., Gölcü, 2019, A. Crystal structure and DNA binding properties of khellin oxime, Journal of Molecular Structure, 1197, 450-457.
[12] Benesi, H.A., Hildebrand, J.H., 1949, A spectrophotometric investigation of the interaction of iodine with aromatic hydrocarbons, J. Am. Chem. Soc. 71, 2703–2707.
[13] Demirezen, N, Tarınç, D, Polat, D, Cemse, M, Gölcü, A., 2012, Tümer, M, Synthesis of trimethoprim metal complexes: Spectral, electrochemical, thermal, DNA-binding and surface morphology studies. Spectrochim. Acta. A. Mol. Biomol. Spectrosc, 94:243–255.
[14] Tarinc, D., Golcu, A., Tumer, M., Karaoglu, T., Ozsoz, M. 2013, Electrochemical investigation and DNA-binding studies of valacyclovir-copper(II) complex, Synthesis and Reactivity in Inorganic, Metal-Organic and Nano-Metal Chemistry, 43, 140-148.
[15] Golcu, A., 2014, Ofloxacin Metal Complexes: Synthesis, Characterization, Analytical Properties, and DNA Binding Studies. Synth. React. Inorganic, Met. Nano-Metal Chem. 44, 1509–1520.
[16] Bekar-Yıldırmaz, B., Şenel, P., Erdoğan, T., Altay, F., Gölcü, A., 2023, Mechanism of interactions of dsDNA binding with quercetin and its two novel sulfonate derivatives using multispectroscopic, voltammetric, and molecular docking studies, Journal of Molecular Structure, 1276, 134718.
[17] Stern, O., Volmer, M., 1919, Phys. Z., 20,183–188.
[18] Cheraghi, S., Şenel, P., Topal, B.D., Agar, S., Majidian, M., Yurtsever, M., Atici, E.B., Gölcü, A., Ozkan, S.A., 2023, Elucidation of DNA-Eltrombopag Binding: Electrochemical, Spectroscopic and Molecular Docking Techniques, Biosensors 13(3), 300.
[19] Waihenya, S., Şenel, P., Osonga, F.J., Erdoğan, T., Altay, F., Gölcü, A., Sadik, O.A., 2021, Mechanism of Interactions of dsDNA Binding with Apigenin and Its Sulfamate Derivatives Using Multispectroscopic, Voltammetric, and Molecular Docking Studies, ACS Omega, 6, 5124–5137.
[20] Ponkarpagam, S., Mahalakshmi, G., Vennila, K. N., Elango, K. P., 2020, Multi-spectroscopic, voltammetric and molecular docking studies on binding of anti-diabetic drug rosigiltazone with DNA. Spectrochim. Acta, Part A, 234, 118268.